Metformin and liraglutide ameliorate high glucose-induced oxidative stress via inhibition of PKC-NAD(P)H oxidase pathway in human aortic endothelial cells

バトチュルーン, バトツェツェグ

https://doi.org/10.15017/1470539

出版情報：九州大学, 2014, 博士（医学）, 課程博士
バージョン：
権利関係：全文ファイル公表済

Metformin and liraglutide ameliorate high glucose-induced oxidative stress via inhibition of PKC-NAD(P)H oxidase pathway in human aortic endothelial cells

Authors and affiliations

Battsetseg Batchuluun[a], Toyoshi Inoguchi[a,b], Noriyuki Sonoda[a,b], Shuji Sasaki[a], Tomoaki Inoue[a], Yoshinori Fujimura[b], Daisuke Miura[b], Ryoichi Takayanagi[a]

[a]Department of Internal Medicine and Bioregulatory Science, Graduate School of Medical Sciences, Kyushu University, 3-1-1 Maidashi, Higashi-ku, Fukuoka 812-8582, Japan

[b]Innovation Center for Medical Redox Navigation, Kyushu University, 3-1-1 Maidashi, Higashi-ku, Fukuoka 812-8582, Japan

Corresponding author

Toyoshi Inoguchi, M.D., Ph.D

Department of Internal Medicine and Bioregulatory Science

Graduate School of Medical Sciences, Kyushu University, Fukuoka 812-8582, Japan

Fax: +81-92-642-5287 / Tel: +81-92-642-5284

E-mail: toyoshi@intmed3.med.kyushu-u.ac.jp

Abstract word count: 250

Manuscript word count: 3999

Table/Figure: 0/5

Supplementary figure/movie: 1/3

Graphical abstract: included

Abstract

Objective: Metformin and glucagon like peptide-1 (GLP-1) prevent diabetic cardiovascular complications and atherosclerosis. However, the direct effects on hyperglycemia-induced oxidative stress in endothelial cells are not fully understood. Thus, we aimed to evaluate the effects of metformin and a GLP-1 agonist, liraglutide on high glucose-induced oxidative stress.

Methods: Production of reactive oxygen species (ROS), activation of protein kinase C (PKC) and NAD(P)H oxidase, and changes in signaling molecules in response to high glucose exposure were evaluated in human aortic endothelial cells with and without treatment of metformin and liraglutide, alone or in combination. PKC-NAD(P)H oxidase pathway was assessed by translocation of GFP-fused PKCβ2 isoform and GFP-fused p47 phox, a regulatory subunit of NAD(P)H oxidase, in addition to endogenous PKC phosphorylation and NAD(P)H oxidase activity.

Results: High glucose-induced ROS overproduction was blunted by metformin or liraglutide treatment, with a further decrease by a combination of these drugs. Exposure to high glucose caused PKCβ2 translocation and a time-dependent phosphorylation of endogenous PKC but failed to induce its translocation and phosphorylation in the cells treated with metformin and liraglutide. Furthermore, both drugs inhibited p47 phox translocation and NAD(P)H oxidase activation, and prevented the high glucose-induced changes in intracellulalr diacylglycerol (DAG) level and phosphorylation of AMP-activated protein kinase (AMPK). A combination of these drugs further enhanced all of these effects.

Conclusions: Metformin and liraglutide ameliorate high glucose-induced oxidative stress by inhibiting PKC-NAD(P)H oxidase pathway. A combination of these two drugs provides augmented protective effects, suggesting the clinical usefulness in prevention of diabetic vascular complications.

Keywords

AMPK · DAG · Endothelial cell· High glucose · Liraglutide · Metformin · Oxidative stress · PKC

1. Introduction

Diabetes mellitus has become a diagnosis of considerable and ominous importance in cardiovascular medicine, related to numerous hospital readmissions and high mortality and morbidity. Premature atherosclerosis contributes to 75% of deaths among diabetic patients [1, 2]. The early site at which diabetic macrovascular complications develop is the endothelium. A causal link has been established between high glucose concentration and endothelial cell damage through an overproduction of ROS by multiple biochemical pathways [3-7]. Among them, PKC-dependent activation of NAD(P)H oxidase is considered to be one of the major sources for high glucose-induced ROS overproduction [5-7]. A therapeutic approach that is capable of preventing oxidative stress might be important to reduce the risk of diabetic cardiovascular events. Several clinical trials have found that metformin, a widely used glucose-lowering drug, is associated with decreased cardiovascular mortality [8, 9]. Additionally, a number of studies have shown a reduced production of ROS by metformin treatment [10, 11]; however, the precise mechanism responsible for this effect is still controversial.

GLP-1 is an incretin hormone secreted by the distal intestinal L cell. Based on its various biological properties [12-15], incretin-based drugs aim to increase and maintain the concentration of GLP-1, such as using its analogs and inhibitors of DPP4, the enzyme that degrades GLP-1. Recently, several studies have demonstrated the protective effects of GLP-1 on cardiovascular function [15-17]. In patients with diabetes, it has been shown that GLP-1R agonist exenatide suppresses markers of inflammation, high sensitivity to C-reactive protein and monocyte chemo-attractant protein-1 and improves diabetes-induced endothelial dysfunction [17]. As for the effect of GLP-1 analogue on oxidative stress, Shiraki et al. reported that liraglutide decreased tumor necrosis factor-α-induced oxidative stress in endothelial cells [18]. However, hyperglycemia is the hallmark of diabetes, there is yet lack of study that evaluated the effect of GLP-1 on high glucose-induced oxidative stress. Thus, we aimed to examine the effects of metformin and liraglutide on high glucose-induced oxidative stress and explore underlying mechanisms.

2. Research Design and Methods

2.1 Reagents

Complete information of reagents used in the present study is provided in the supplementary methods.

2.2 Cell Culture

Human aortic endothelial cells (HAECs) were purchased at passage 3 from Lonza (Walkersville, MD, USA). Cells were grown in endothelial growth medium (Clonetics™ EGM™-2 BulletKit™, Lonza) that contained endothelial basal medium supplemented with 2% fetal bovine serum (FBS), hydrocortisone, hFGF-B, VEGF, R3-IGF-1, ascorbic acid, hEGF, GA-1000 and heparin. The culture was maintained at 37°C under 5% of humidified atmosphere until confluence. All of the experiments were performed at passage 6. After reaching confluence, the culture conditions were changed to a test medium that contained 20% endothelial growth medium and 80% endothelial basal medium and incubated for 48 h before proceeding with further experiments.

2.3 Plasmid Construction and Transfection

HAECs were seeded in 35-mm glass-bottom dishes at a density of 5×10^4 cells per well and grown until confluence. After lipofection optimization was completed, lipofection was performed by diluting Lipofectamine LTX (2 μl), PLUS Reagent (0.5 μl) and the plasmid (500 ng) in Opti-MemI medium (25 μl) and adding the mixture into the confluent cell culture under test medium conditions. pGFP3 with no insert was used as an empty vector control. The C1 domain of conventional PKC functions as a DAG-/phorbol-binding site [19, 20]. To delete this domain, two sets of primer pairs were designed: 5'-AAG CTT GCC ACC ATG GAA TTC GGA TCC-3' (forward primer-1), 5'-TTT CTC GAG CTT CAC CTC GTG CAC GTT-3' (reverse primer-1) and 5'-GGA CTC GAG TAT ATC CAG GCC CAC ATC G-3' (forward primer-2), 5'-GAC CGG TGG ATC GGA TCC GCT CTT GAC-3' (reverse primer-2). These

primers bound to the sequences before and after the DAG-binding site separately as the following restriction site fragments: upper strands: EcoRI or XhoI and lower strands: XhoI or BamHI fragments were subcloned, respectively. Using the restriction sites, ligation was first performed using the DNA ligation kit between the two cloned sequences and then between the ligated sequence and the pGFP3 vector. Deletion of the DAG-binding site was confirmed by sequence analysis. To construct the p47phox-pGFP3 plasmid, we designed one primer pair where a restriction site, EcoRI, was subcloned in either strand: CAC GAA TTC GGG GAC ACC TTC ATC CGT (forward primer) and GTT GAA TTC GAC GGC AGA CGC CAG CTT (reverse primer). The cloned product was cut by EcoR1 enzyme and ligated into the pGFP3 vector. Direction and sequence of p47phox-pGFP3 plasmid construction was confirmed by sequence analysis.

2.4 Translocation Experiment

Twenty-four hours after lipofection, 1 μg/ml of Hoechst 33258 was added to the cells to stain the nucleus. After 30 min of incubation, the cells were placed on a heated microscopy plate at 37°C under a 5% humidified atmosphere and stimulated with 25 mM D-glucose or positive controls as follows: 32.4 nM PMA and 5 μM histamine. An empty pGFP3 vector with 25 mM D-glucose stimulation and either PKCβ2-pGFP3 or a p47 phox-pGFP3 vector with 25 mM D-mannitol added were used for the negative controls. Time-series imaging of the GFP signaling was recorded by A1Rsi confocal microscopy (Nikon, Tokyo, Japan) at excitation and emission wavelengths of 488 and 525 nm, respectively. To quantify the changes in the fluorescence intensity of GFP in the cell membrane and cytosol during translocation, region of interest (ROI) was defined by gating the cell membrane and cytosol, separately and tracked over time during the time-series imaging (NIS-Elements AR 4.00.03 Advanced Software, Nikon, Japan). Translocated GFP was determined by the measured ROI intensity and calculated as a ratio of ROI intensity of the membrane to that of cytosol.

2.5 ROS Detection

ROS production was measured by dihydroethidium (DHE) staining. HAECs were seeded in 48-well plates at a density of 1×10^4cells/well and incubated until confluent in endothelial growth medium. Subsequently, the culture conditions were changed to test medium where the cells were further incubated for 48 h before stimulation. DHE was added at a final concentration of 10 μM, and the cells were incubated at 37°C under 5% of humidified atmosphere to stain. After 60 min, the cells were washed with room temperature PBS twice and placed under fluorescence microscopy (model BZ-9000; Keyence, Osaka, Japan). Images were captured in a dark chamber at excitation and emission wavelengths of 560 and 630 nm, respectively. The fluorescence intensity was quantified using BZ image analysis software (Keyence, Osaka, Japan).

2.6 Western Blotting Analysis

HAECs were seeded in 6-well plates at a density of 1×10^5 cells/well. After reaching confluence, the cells were preincubated in the test medium for 48 h before further experiments. The cells were lysed in lysis buffer (50 mM Tris-HCl, pH 7.4, 150 mM NaCl, 5 mM sodium fluoride, 0.25 mM EDTA, pH 8.0, 1% deoxycholic acid, 1% Triton X-100 and 1 mM sodium orthovanadate) supplemented with a protease inhibitor mixture (Sigma) and phosphatase inhibitors (Sigma). The samples were then separated on 10% SDS-polyacrylamide gels (Bio-Rad) and transferred onto 0.2-μm polyvinyl difluoride membranes (Bio-Rad) in Tris/glycine buffer. The membranes were exposed to primary antibodies followed by HRP-conjugated secondary antibodies. The signals were detected using a chemiluminescent reaction (ECL Plus, Amersham Biosciences). The primary antibodies used were phosphospecific anti-pan-PKC rabbit monoclonal antibody (1:1000), anti-pan-PKC rabbit polyclonal antibody, phosphospecific anti-AMPK rabbit polyclonal antibody (1:1000), anti-AMPK rabbit polyclonal antibody (1:1000), and anti-β-actin mouse polyclonal antibody (1:10 000).

2.7 Measurement of Intracellular DAG

HAECs were seeded in a 10-cm dish at a density of 4×10^5 cells per dish and grown in 4% FBS medium. After high glucose (25mM) exposure for 1 h with and without 1 h of pre-incubation with metformin (10 μM) and/or liraglutide (30 nM) and 5-Aminoimidazole-4-carboxamide ribonucleotide (AICAR) (0.1 mM), the cells were lysed by methanol, and subsequently total lipids were extracted using Folch's method [21]. Total diacylglycerol content and various molecular species of diacylglycerol were measured using high performance liquid chromatography (HPLC)-tandem mass spectrometry as previously described [22, 23].

2.8 Lucigenin-Enhanced Chemiluminescence (LEC) Assay

NAD(P)H oxidase activity was evaluated by an LEC assay as previously described [24]. Briefly, HAECs were subcultured into 25-cm^2 collagen type 1-coated culture flasks at a density of 1.2×10^5 cells per flask. When the cultures reached confluence, they were further incubated for 48 h in test medium, containing 5.5mM basal glucose before performing the assay. After high glucose stimulation (25mM) with and without 1h pre-treatment, the cells were detached using HEPES, trypsin/EDTA and a trypsin-neutralizing solution. The cells were resuspended in LEC assay buffer that contained NaCl (140 mM), KCl (5 mM), $MgCl_2{\cdot}6H_2O$ (0.8 mM), $CaCl_2{\cdot}2H_2O$ (1.8 mM), $Na_2HPO_4{\cdot}12H_2O$ (1 mM), HEPES (25 mM) and glucose (1%). The cells were distributed at 2.5×10^5/well on a 96-well microplate luminometer (LB960 Centro, Berthold, Germany) and lucigenin at a final concentration of 10 μM was added. The reaction was initiated with the addition of NADPH (100 μM) after recording the background for 5 min. Light emission was recorded and expressed as mean relative light units (RLU) for 60 min to minimize artificial superoxide anion production owing to redox cycle.

2.9 ***Statistical analysis***

Data are reported as the mean±SE. An unpaired Student *t*-test was used to detect significant differences when two groups were compared and an anova test followed by post-host tests was used when more than two groups were compared. Significance was considered when $p<0.05$.

3. Results

3.1 Augmented effect of metformin and liraglutide on inhibition of high glucose-induced ROS overproduction

ROS generation was measured by DHE staining in the cells incubated with normal glucose and high glucose conditions. Incubation of the cells with high glucose resulted in increased production of ROS (185.4±30.8% vs. 100% of control, $p<0.001$, Fig. 1A and B). High glucose-induced ROS overproduction was blunted in the cells treated with metformin (10μM) and liraglutide (30 nM) alone at therapeutic blood concentrations, up to 115.5±22.0% and 112.7±24.7%, respectively. Moreover, their combination treatment resulted in a further decrease of ROS levels up to 99.2±19.6%. The cell viability was over 94% in each sample (Supplementary Fig.1). To understand the source of the high glucose-induced ROS production, we determined the effect of calphostin C, a PKC inhibitor, and apocynin, a NAD(P)H oxidase inhibitor. The effect of high glucose on ROS production was also abolished by calphostin C and apocynin.

3.2 High glucose caused PKCβ2 translocation and endogenous PKC phosphorylation

PKCβ isoform was reported to be preferentially increased in both the aorta and heart of diabetic rats; and endothelial cells of diabetic patients [25-29]. To evaluate PKCβ activity, PKCβ2-pGFP3 vector was transfected and its translocation was captured in time-series imaging. PKCβ2-pGFP3 translocation to the cell membrane was observed within 1 h after the addition of 25 mM D-glucose (Fig. 2A, B and Supplemental Movie. 1). 32.4 nM PMA was used for a positive control, which induced PKCβ2 translocation within 20 min after stimulation (Fig. 2C, D and Supplemental Movie. 2), whereas there was no translocation observed in negative controls, an empty pGFP3 vector with stimulation of 25mM D-Glucose (Fig. 1E, F and Supplemental Movie. 3) and PKCβ2-pGFP3 vector with the addition of 25 mM D-mannitol (data not shown). Furthermore, we observed a time-dependent increase of endogenous PKC phosphorylation in response to high glucose stimulation (Fig. 2G).

3.3 DAG-binding site is important in high glucose-induced PKCβ translocation

Conventional PKC isoforms contain both DAG/phorbol- and calcium-binding sites in the regulatory domain. Translocation of PKC is initiated by the substrate molecules through specifically binding to these sites. To assess the importance of DAG-binding site in high glucose-induced PKC translocation, we constructed a mutant PKCβ2-pGFP3 plasmid in which DAG-binding site was deleted. The complete vector sequence of PKCβ2-pGFP3 was translocated into the cell membrane in response to high glucose exposure (Fig. 3A and B), whereas there was no translocation of the mutant-PKCβ2-pGFP3 was observed in high glucose condition (Fig. 3C and D). However, the mutant-PKCβ2-pGFP3 was promptly translocated into the cell membrane in response to 5 μM histamine addition in the same cells. Previously, histamine was shown to release intracellular calcium level and induce PKC translocation [30, 31]. In our study, the mutant-PKCβ2-pGFP3 was capable of translocating in response to histamine but it was prevented in high glucose stimulation. Thus, DAG-binding site might be essential in high glucose-induced PKCβ2 translocation.

3.4 Metformin and liraglutide prevented high glucose-induced DAG increase

Next, we determined whether there is an increase in intracellular DAG levels preceding PKCβ2 translocation. Total DAG was significantly increased in the cells incubated with high glucose compared with normal glucose (Fig. 3E). We previously reported that the composition of DAG derived from glycolytic *de novo* synthesis shows a predominance of palmitate and oleate. Therefore, among various DAGs, we evaluated 1-palmitoyl-2oleoyl-glycerol, 1,2-dipalmitoyl-glycerol and 1,2-dioleoyl-glycerol concentrations by HPLC-tandem mass spectrometry. Treatment with metformin and liraglutide resulted in a significant reduction of those DAGs (Fig. 3F, G and H), and a combination of metformin and liraglutide appeared to further decrease 1,2-dipalmitoyl-glycerol concentrations (0.032±0.006 pmol and 1.13±0.34 pmol per μg total protein, respectively, $p<0.05$, Figure 3G). Previously, glucose incorporation into DAG

was shown to be inhibited by AMPK activation [32]. To verify whether the reduction of DAG in the present study is mediated through modulating AMPK activation, we tested an AMPK activator, AICAR for a positive control which also caused a significant decrease of those DAGs (Fig. 3E-H).

3.5 Protective effect of metformin and liraglutide on AMPK phosphorylation and PKC activation

We next examined AMPK phosphorylation in metformin- and/or liraglutide-treated conditions. There was a significant decrease in AMPK phosphorylation in the high glucose-stimulated cells, whereas pre-treatment with metformin and liraglutide prior to high glucose stimulation restored AMPK phosphorylation (Fig. 4A). Moreover, this effect was enhanced with a combined pre-treatment of these drugs. We also determined whether metformin and liraglutide in combination has a complementary effect on PKC phosphorylation. Both metformin and liraglutide suppressed PKC phosphorylation and this effect was augmented with a combination treatment of these drugs (Fig. 4B). The finding that metformin and liraglutide reduced PKC phosphorylation was consistent with their inhibitory effect on PKCβ2-pGFP3 translocation shown by the GFP intensity ratio of membrane to cytosol before and after high glucose exposure or PMA addition into same cells (Fig. 4C).

3.6 Metformin and liraglutide inhibited p47phox translocation and NAD(P)H oxidase activation caused by high glucose

We further evaluated the effect of metformin and liraglutide on NAD(P)H oxidase activity. In the unstimulated cells, p47 phox-pGFP3 was located in the cytosol, and it was translocated into the cell membrane in response to high glucose stimulation (Fig. 5A and B) or 32.4 nM PMA (data not shown). Pre-incubation with metformin (Fig. 5C and D) or liraglutide (Fig. 5E and F) prevented high glucose-induced translocation of p47 phox-pGFP3. However, after subsequent addition of 5 μM histamine into the same cells, p47 phox-pGFP3 was translocated to the cell membrane. We also evaluated NAD(P)H oxidase activity by an LEC assay. In consistent with p47phox translocation, high glucose levels

were shown to increase NAD(P)H oxidase activity, whereas metformin and liraglutide prevented high glucose-induced activation with a further decrease of NAD(P)H oxidase activity in a combination treatment. AICAR also decreased NAD(P)H oxidase activity (Fig. 5G).

4. Discussion

This study findings demonstrated that both metformin and liraglutide prevent high glucose-induced oxidative stress through inhibition of PKC-NAD(P)H oxidase pathway in cultured human endothelial cells. In addition, we found an augmented effect of metformin and liraglutide on reducing high glucose-induced oxidative stress, suggesting the clinical usefulness of a combination treatment of these drugs. Of particular note on the present study is that the finding that these two drugs work in a similar manner through affecting same signaling molecules, AMPK and intracellular DAG in endothelial cells.

We and other investigators have shown that PKCβ isoform was increased in the aorta and heart of diabetic rats, and in endothelial cells of diabetic patients, causing various dysfunctions in diabetic vascular tissues [25-29]. In this study, to evaluate the activity of PKCβ, GFP-fused PKCβ2 were transfected into the cells. As for the NAD(P)H oxidase activity, its regulatory subunit p47phox was also transfected into the cells. Preceding the ROS elevation, high glucose levels were shown to induce translocation of PKCβ2 and p47phox, and the time point was also compatible with the increases in endogenous PKC phosphorylation and NAD(P)H oxidase activity. These findings were consistent with our previous report showing that high glucose stimulates ROS production mainly through an activation of the PKC-NAD(P)H pathway rather than mitochondria [5]. Using these assay systems, we found that metformin was capable of inhibiting PKCβ translocation at a concentration of 10 μM with a 1-h pre-incubation time. The present study found for the first time that liraglutide at a concentration of 30 nM for a 1-h pre-incubation time also inhibited high glucose-induced PKCβ translocation. These results were consistent with the decreased phosphorylation of endogenous PKC in both metformin- and liraglutide-treated cells. Furthermore, we have shown that translocation of p47phox induced by high glucose levels was inhibited by both

metformin and liraglutide treatment. Similarly, NAD(P)H oxidase activity was increased by high glucose levels, and this increase was inhibited by both metformin and liraglutide treatment.

A number of studies have reported that DAG levels were increased in the aorta and heart of diabetic rats and in high glucose-stimulated cultured aortic endothelial cells through glycolytic *de novo* DAG synthesis [25, 33, 34]. The C1 domain of conventional PKC isoforms that functions as a DAG-/phorbol-binding site is important for PKC translocation and phosphorylation [31, 32]. We found that a mutant PKCβ that lacks DAG/binding site was capable of translocating by another stimulus, histamine, but it was not translocated in response to high glucose stimulation, providing direct evidence that DAG might be necessary for high glucose-induced PKCβ activation. It was previously demonstrated that factors that activate AMPK, such AICAR and metformin, increase fatty acid oxidation by affecting enzymes that govern malonyl CoA synthesis and possibly its degradation, and decrease triglyceride synthesis in the adipocyte and other cells [35]. Ido et al. reported that a high glucose-induced increase in endothelial cell apoptosis was preceded by inhibition of fatty acid oxidation, by an increase in DAG synthesis and concentrations of malonyl CoA, and by a decrease in mitochondrial membrane potential and cellular ATP content, and all of these changes were completely prevented by incubation with AICAR [32]. The present study revealed that both metformin and liraglutide increased AMPK phosphorylation, suggesting that the inhibiting effect on PKC activity of these two drugs might be due to decreased *de novo* DAG synthesis by the activation of AMPK. This hypothesis was supported by the findings that metformin and liraglutide reduced total DAG levels including 1-palmitoyl-2-oleoyl-glycerol, 1,2-dipalmitoyl-glycerol and 1,2-dioleoyl-glycerol, which was also consistent with our previous finding that the fatty acid composition of DAG derived from high glucose-induced *de novo* synthesis shows a predominance of palmitate and oleate [25, 29].

Several studies have shown that high glucose levels decrease AMPK phosphorylation in rat red muscles and liver [36]. In our study, AMPK phosphorylation was also decreased in endothelial cells incubated with high glucose conditions. Considering the fact that AMPK is a cellular energy sensor [37, 38], we

primarily assumed that it might be related to a change in the cellular energy state after acute exposure to high glucose. However, in contrast, ATP concentrations were shown to be unchanged after such acute exposure to high glucose for 1 h (data not shown), suggesting that there could be an ATP-independent mechanism suppressing AMPK phosphorylation. The effect of liraglutide on AMPK activation is possibly due to an increase in intracellular cAMP levels. A recent study has demonstrated that similar to the action of GLP-1 on cAMP induction observed at physiological glucose concentration, GLP-1 retained its ability to stimulate cAMP generation at 30mM glucose and produced 1.6-fold increase in cAMP levels [39]. Considerable evidence linking the increased cAMP and AMPK has indicated that cAMP induction promotes AMPK phosphorylation in PKA- and Epac1-dependent manners [40, 41].

A recent study identified that GLP-1 has a protective effect on the glomerular endothelium, but its effect was diminished by increased GLP-1 receptor degradation due to diabetes-induced PKCβ2 activation [42]. Although there was no significant alteration of GLP-receptor (GLP-1R) expression in exposure to high glucose levels for 1 h in our study (data not shown), a combination therapy of metformin with incretin-based drugs, such as liraglutide, may be preferable in the clinical practice for preventing increased GLP-1R degradation caused by PKCβ2 activation, thereby improving the protective effect of GLP-1 because metformin showed an inhibitory effect on PKCβ2 activity.

In conclusion, this study demonstrated the protective effects of metformin and liraglutide against high glucose-induced oxidative stress by inhibiting PKC-NAD(P)H oxidase pathway in endothelial cells (graphical abstract). It might be beneficial in delaying endothelial damage in diabetic vessels and contributing reduced risk of diabetic cardiovascular complications. This protective effect was augmented in combination of these drugs, suggesting a promising treatment option in prevention of diabetic vascular complications. It needs to be confirmed by further studies in clinical practice.

Conflict of interest

The authors have no conflict of interest to report in relation to this manuscript.

Acknowledgment

This work was supported in part by the Special Coordination Funds for Promoting Science and Technology (SCF funding program “Innovation Center for Medical Redox Navigation”). We appreciate the technical support from the Research Support Center, Graduate School of Medical Sciences, Kyushu University.

References

[1] American Diabetes association. Consensus Statement: Role of cardiovascular risk factors in prevention and treatment of macrovascular disease in diabetes. Diabetes Care 1993, 16:72-78.

[2] Members ATF, Ryden L, Standl E et al. Guidelines on diabetes, pre-diabetes, and cardiovascular disease. Eur Heart J Suppl 2007; 9(Suppl C): C3–74.

[3] Hunt JV, Dean RT, Wolff SP. Hydroxyl radical production and autoxidative glycosylation. Glucose autoxidation as the cause of protein damage in the experimental glycation model of diabetes mellitus and ageing. Biochem J 1988;256:205-212.

[4] Nishikawa T, Edelstein D, Du XL, et al. Normalizing mitochondrial superoxide production blocks three pathways of hyperglycaemic damage. Nature 2000;404:787-790.

[5] Inoguchi T, Li P, Umeda F, et al. High glucose level and free fatty acid stimulate reactive oxygen species production through protein kinase C-dependent activation of NAD(P)H oxidase in cultured vascular cells. Diabetes 2000;49:1939-1945.

[6] Inoguchi T, Sonta T, Tsubouchi H, et al. Protein kinase C-dependent increase in reactive oxygen species (ROS) production in vascular tissues of diabetes: role of vascular NAD(P)H oxidase. J Am Soc Nephrol 2003;14:S227-232.

[7] Kim YK, Lee MS, Son SM, et al. Vascular NADH oxidase is involved in impaired endothelium-dependent vasodilation in OLETF rats, a model of type 2 diabetes. Diabetes 2002;51:522-527.

[8] UK Prospective Diabetes Study (UKPDS) Group. Effect of intensive blood-glucose control with metformin on complications in overweight patients with type 2 diabetes (UKPDS 34). Lancet 1998;352:854-865.

[9] UK Prospective Diabetes Study (UKPDS) Group. Intensive blood-glucose control with sulphonylureas or insulin compared with conventional treatment and risk of complications in patients with type 2 diabetes (UKPDS 33). Lancet 1998;352:837-853.

[10] Gallo A, Ceolotto G, Pinton P, et al. Metformin prevents glucose-induced protein kinase C-beta2 activation in human umbilical vein endothelial cells through an antioxidant mechanism. Diabetes 2005;54:1123-1131.

[11] Ouslimani N, Peynet J, Bonnefont-Rousselot D, et al. Metformin decreases intracellular production of reactive oxygen species in aortic endothelial cells. Metabolism 2005;54:829-834.

[12] Lovshin JA, Drucker DJ. Incretin-based therapies for type 2 diabetes mellitus. Nat Rev Endocrinol 2009;5:262-269.

[13] Fadini GP, Simioni N, Frison V, et al. Independent glucose and weight-reducing effects of Liraglutide in a real-world population of type 2 diabetic outpatients. Acta Diabetol. 2013; ahead of print.

[14] Fadini GP, Avogaro A. Cardiovascular effects of DPP-4 inhibition: beyond GLP-1. Vascul Pharmacol. 2011;55(1-3):10-6.

[15] Nagashima M, Watanabe T, Terasaki M, et al. Native incretins prevent the development of atherosclerotic lesions in apolipoprotein E knockout mice. Diabetologia 2011;54:2649-2659.

[16] Arakawa M, Mita T, Azuma K, et al. Inhibition of monocyte adhesion to endothelial cells and attenuation of atherosclerotic lesion by a glucagon-like peptide-1 receptor agonist, exendin-4. Diabetes 2010;59:1030-1037.

[17] Koska J, Schwartz EA, Mullin MP, et al. Improvement of postprandial endothelial function after a single dose of exenatide in individuals with impaired glucose tolerance and recent-onset type 2 diabetes. Diabetes Care 2010;33:1028-1030.

[18] Shiraki A, Oyama J, Komoda H, et al. The glucagon-like peptide 1 analog liraglutide reduces TNF-α-induced oxidative stress and inflammation in endothelial cells. Atherosclerosis 2012;221:375-382.

[19] Rosse C, Linch M, Kermorgant S, et al. PKC and the control of localized signal dynamics. Nat Rev Mol Cell Biol 2010;11:103-112.

[20] Steinberg SF. Structural basis of protein kinase C isoform function. Physiol Rev 2008;88:1341-1378.

[21] Folch J, Lees M, Sloane Stanley GH. A simple method for the isolation and purification of total lipides from animal tissues. J Biol Chem 1957;226:497-509.

[22] Bielawski J, Szulc ZM, Hannun YA, et al. Simultaneous quantitative analysis of bioactive sphingolipids by high-performance liquid chromatography-tandem mass spectrometry. Methods 2006;39: 82-91.

[23] Inoue T, Kobayashi K, Inoguchi T, et al. Reduced expression of adipose triglyceride lipase enhances tumor necrosis factor alpha-induced intercellular adhesion molecule-1 expression in human aortic endothelial cells via protein kinase C-dependent activation of nuclear factor-kappaB. J Biol Chem 2011;286:32045-32053.

[24] Fujii M, Inoguchi T, Sasaki S, et al. Bilirubin and biliverdin protect rodents against diabetic nephropathy by downregulating NAD(P)H oxidase. Kidney Int 2010;78:905-919.

[25] Inoguchi T, Battan R, Handler E, et al. Preferential elevation of protein kinase C isoform beta II and diacylglycerol levels in the aorta and heart of diabetic rats: differential reversibility to glycemic control by islet cell transplantation. Proc Natl Acad Sci U S A 1992;89:11059-11063.

[26] Ishi H. Amelioration of vascular dysfunction in diabetic rats by an oral PKC beta inhibitor. Science 1996;272:728-731.

[27] Tabit CE, Shenouda SM, Holbrook M, et al. Protein kinase C-β contributes to impaired endothelial insulin signaling in humans with diabetes mellitus. Circulation. 2013;127:86-95.

[28] Kouroedov A, Eto M, Joch H, et al. Selective inhibition of protein kinase C b 2 prevents acute effects of high glucose on vascular cell adhesion molecule-1 expression in human endothelial cells. Circulation J 2004;110:91-96.

[29] Geraldes P, King GL. Activation of protein kinase C isoforms and its impact on diabetic complications. Circ Res 2010;106:1319-1331.

[30] Khankoeva A, Dukhanin A, Galeno-Yaroshevskii P. Mechanism of histamine-induced increase of calcium level in cardiomyocytes. A relative efficacy of histamine receptor blockers. Bull Exp Biol Med 1997; 123(4):357-59

[31] Schaefer M, Albrecht N, Hofmann T, Gudermann T, Schultz G. Diffusion-limited translocation mechanism of protein kinase C isotypes. FASEB J. 2001 Jul;15(9):1634-6.

[32] Ido Y, Carling D, Ruderman N. Hyperglycemia-induced apoptosis in human umbilical vein endothelial cells: inhibition by the AMP-activated protein kinase activation. Diabetes 2002;51:159-167.

[33] Inoguchi T, Pu X, Kunisaki M, et al. Insulin's effect on protein kinase C and diacylglycerol induced by diabetes and glucose in vascular tissues. Am J Physiol 1994;267:369-379.

[34] Pu X, Inoguchi T, Kern TS, et al. Characterization of the mechanism for the chronic activation of diacylglycerol-protein kinase C in diabetes and hypergalactosemia. Diabetes 1994;43:1122-1129.

[35] Ruderman NB, Saha AK, Kraegen EW. Minireview: Malonyl CoA, AMP-activated protein kinase, and adiposity. Endocrinol 2003;144:5166-5171.

[36] Kraegen EW, Saha AK, Preston E, et al. Increased malonyl-CoA and diacylglycerol content and reduced AMPK activity accompany insulin resistance induced by glucose infusion in muscle and liver of rats. Am J Physiol Endocrinol Metab 2006;290:E471-479.

[37] Carling D, Mayer FV, Sanders MJ, et al. AMP-activated protein kinase: nature's energy sensor. Nat Chem Biol 2011;7:512-518.

[38] Schimmack G, Defronzo RA, Musi N. AMP-activated protein kinase: Role in metabolism and therapeutic implications. Diabetes Obes Metab 2006;8:591-602.

[39] Luo G, Kong X, Lu L, et al. Glucagon-like peptide 1 potentiates glucotoxicity-diminished insulin secretion via stimulation of cAMP-PKA signaling in INS-1E cells and mouse islets. Int J Biochem Cell Biol 2013;45:483-490.

[40] Yin W, Mu J, Birnbaum MJ. Role of AMP-activated protein kinase in cyclic AMPdependent lipolysis in 3T3-L1 adipocytes. J Biol Chem 2003;278:43074–43080.

[41] Park SJ, Ahmad F, Philp A, et al. Resveratrol ameliorates aging-related metabolic phenotypes by inhibiting cAMP phosphodiesterases. Cell 2012;148:421–433.

[42] Mima A, Hiraoka-Yamomoto J, Li Q, et al. Protective effects of GLP-1 on glomerular endothelium and its inhibition by PKCβ activation in diabetes. Diabetes 2012;61:2967-2979.

Figure legends

Fig. 1

Metformin and liraglutide ameliorated high glucose-induced ROS overproduction. ROS production in response to high glucose stimulation (25mM) was measured by DHE staining in cultured HAECs pre-treated with metformin (10μM) and liraglutide (30nM), alone and in combination, calphostin C (0.1μM) and apocynin (0.1nM). A: Representative DHE staining images with original magnification x20. B: The fluorescence intensity was calculated and expressed as the means ± SE of three independent experiments; **p<0.01; $^{\#\#}$p<0.01 vs metformin; ¶¶p<0.01 vs liraglutide.

Fig. 2

Effect of high glucose on PKCβ2 translocation and endogenous PKC phosphorylation. PKCβ2-pGFP3

translocation was imaged before and after high glucose exposure (A); before and after PMA stimulation for a positive control (C); before and after high glucose stimulation of empty pGFP3-transfected cells for a negative control (E); Original magnification x40. GFP intensity was calculated by tracking the regions of interest during time-series imaging (B, D and F) and expressed as the means ± SE of three independent experiments. **p<0.01, ns: non-significant; G: A representative figure of western blotting for endogenous PKC phosphorylation in endothelial cells exposed to high glucose for 10; 20; 30; 40; 50; 60; 120 minutes and PMA for 30 minutes (left panel). Densitometry analysis was performed and expressed as means ± SE from three independent experiments (right panel). *p<0.05, **p<0.01.

Fig. 3

DAG is important in high glucose-induced PKCβ2 translocation and it was reduced by metformin and liraglutide. A: Translocation of complete vector sequence PKCβ2-pGFP3 before and after high glucose stimulation; C: mPKCβ2-pGFP3 translocation before and after high glucose stimulation or after histamine addition for a positive control; Original magnification was x40. B and D: GFP intensity was measured by tracking the regions of interest during time-series imaging and expressed as means ± SE of three independent experiments. **p<0.01, ns: non-significant. Total DAG (E), 1-palmitoyl-oleoyl-glycerol (F), 1,2-dipalmitoyl-glycerol (G), 1,2-oleoyl-glycerol (H) were measured and expressed as the means ± SE from five experiments; *p<0.05, **p<0.01, $^{\#}$p<0.05 vs metformin.

Fig. 4

Augmented effect of metformin and liraglutide on phosphorylation of AMPK and PKC. Representative figures of western blotting analysis show AMPK phosphorylation (**A**) and PKC phosphorylation (**B**) in HAECs exposed to high glucose condition with and without metformin and liraglutide treatment, alone or in combination, and AICAR. Densitometry analysis was performed and expressed as means ± SE from three independent experiments; *p<0.05, **p<0.01, $^{\#}$p<0.05 vs metformin. **C**: In time-series imaging

experiments, PKCβ2-pGFP3 translocation was captured and GFP intensity ratio of membrane to cytosol was measured in HAECs before and after high glucose exposure or PMA addition into the same cells under untreated, metformin-treated and liraglutide-treated conditions. Data are the means ± SE of three independent experiments. **p<0.01, ns: non-significant.

Fig. 5

Metformin and liraglutide suppressed high glucose-induced NAD(P)H oxidase activation. p47phox-pGFP3 vector localization was captured before and after high glucose stimulation in the untreated cells (A); before and after high glucose exposure and after subsequent addition of histamine in the metformin-treated cells (C) and liraglutide-treated cells (E); Original magnification was x40. GFP intensity was calculated by tracking the regions of interest during time-series imaging in the untreated (B), metformin-treated (D) and liraglutide-treated (F) cells. Data are the means ± SE of three independent experiments. **p<0.01, ns: non-significant. G: NAD(P)H oxidase activity was measured by LEC assay and fluorescence intensity was expressed as the means ± SE of five independent experiments; *p<0.05, ¶ p<0.05 vs liraglutide.

Fig. 1

A

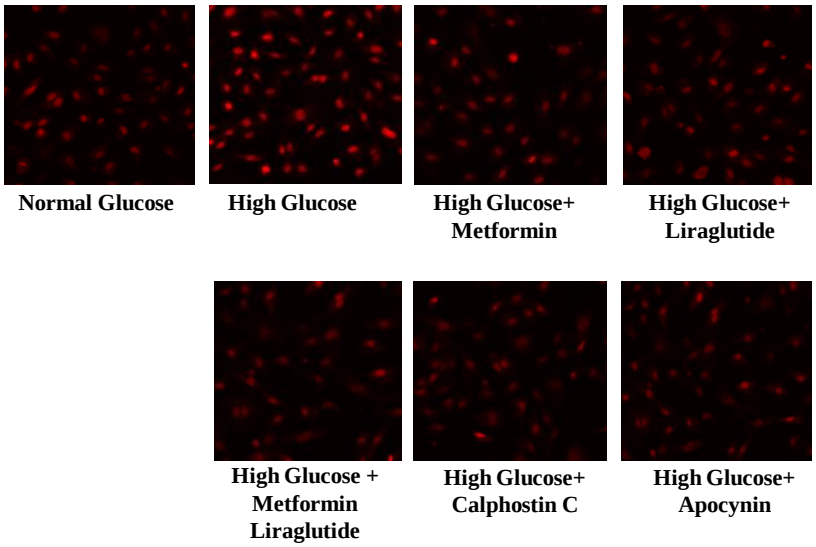
Normal Glucose
High Glucose
High Glucose+ Metformin
High Glucose+ Liraglutide
High Glucose + Metformin Liraglutide
High Glucose+ Calphostin C
High Glucose+ Apocynin

B

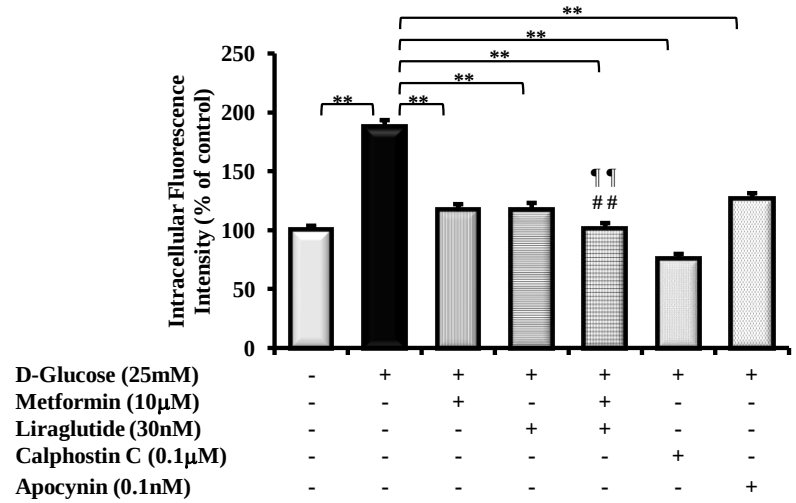
Intracellular Fluorescence Intensity (% of control)
250
200
150
100
50
0
**
**
**
**
**
**
¶ ¶
# #
D-Glucose (25mM) - + + + + + +
Metformin (10μM) - - + - + - -
Liraglutide (30nM) - - - + + - -
Calphostin C (0.1μM) - - - - - + -
Apocynin (0.1nM) - - - - - - +

Fig. 2

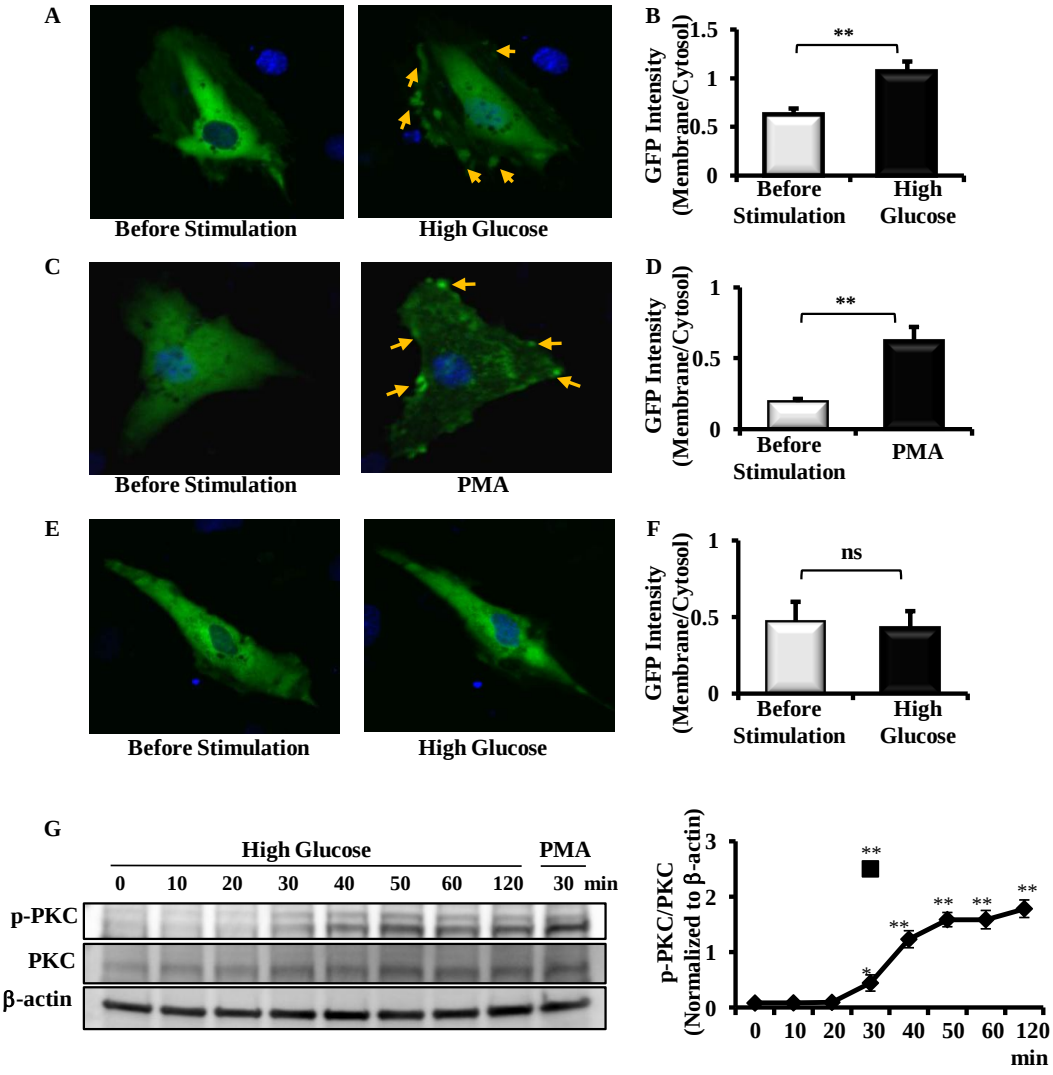
A
Before Stimulation
High Glucose
B
GFP Intensity (Membrane/Cytosol)
1.5
1
0.5
0
**
Before Stimulation
High Glucose
C
Before Stimulation
PMA
D
GFP Intensity (Membrane/Cytosol)
1
0.5
0
**
Before Stimulation
PMA
E
Before Stimulation
High Glucose
F
GFP Intensity (Membrane/Cytosol)
1
0.5
0
ns
Before Stimulation
High Glucose
G
High Glucose
PMA
0 10 20 30 40 50 60 120 30 min
p-PKC
PKC
β-actin
p-PKC/PKC (Normalized to β-actin)
3
2
1
0
**
*
0 10 20 30 40 50 60 120
min

Fig. 3

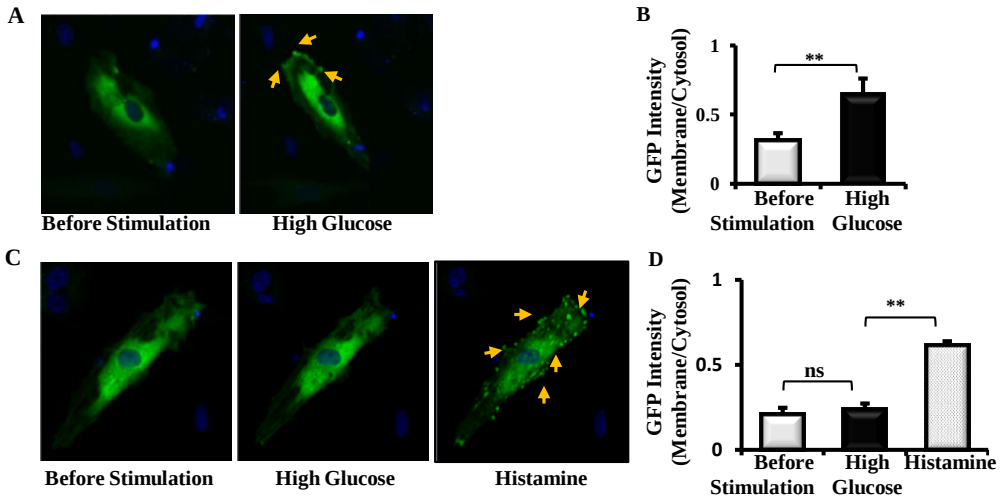
A
Before Stimulation
High Glucose
B
GFP Intensity (Membrane/Cytosol)
Before Stimulation
High Glucose
C
Before Stimulation
High Glucose
Histamine
D
GFP Intensity (Membrane/Cytosol)
ns
Before Stimulation
High Glucose
Histamine

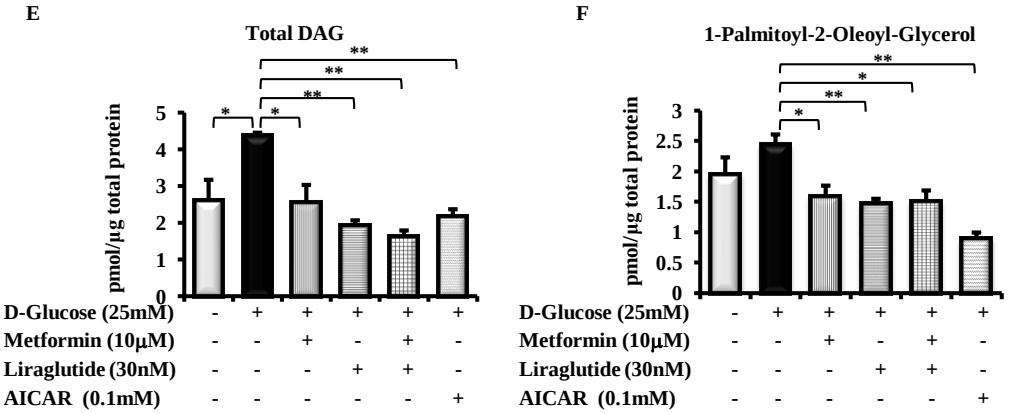
E
Total DAG
pmol/μg total protein
D-Glucose (25mM)
Metformin (10μM)
Liraglutide (30nM)
AICAR (0.1mM)
F
1-Palmitoyl-2-Oleoyl-Glycerol
pmol/μg total protein
D-Glucose (25mM)
Metformin (10μM)
Liraglutide (30nM)
AICAR (0.1mM)

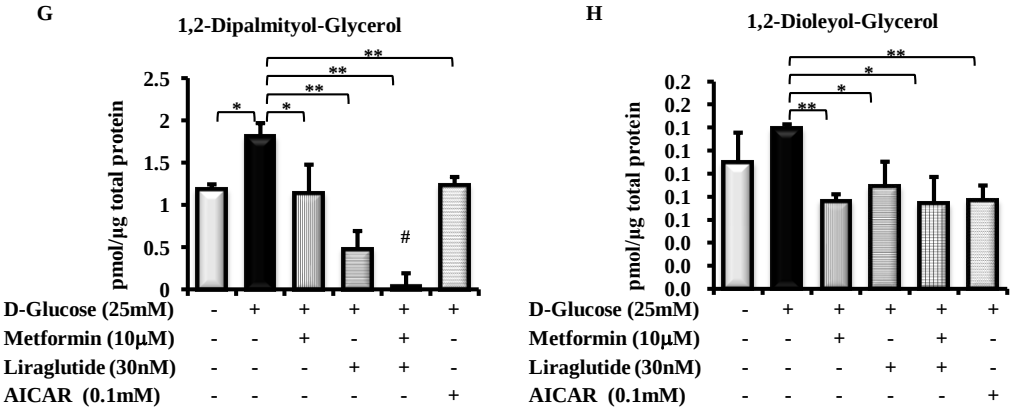
G
1,2-Dipalmityol-Glycerol
pmol/μg total protein
D-Glucose (25mM)
Metformin (10μM)
Liraglutide (30nM)
AICAR (0.1mM)
H
1,2-Dioleyol-Glycerol
pmol/μg total protein
D-Glucose (25mM)
Metformin (10μM)
Liraglutide (30nM)
AICAR (0.1mM)

Fig. 4

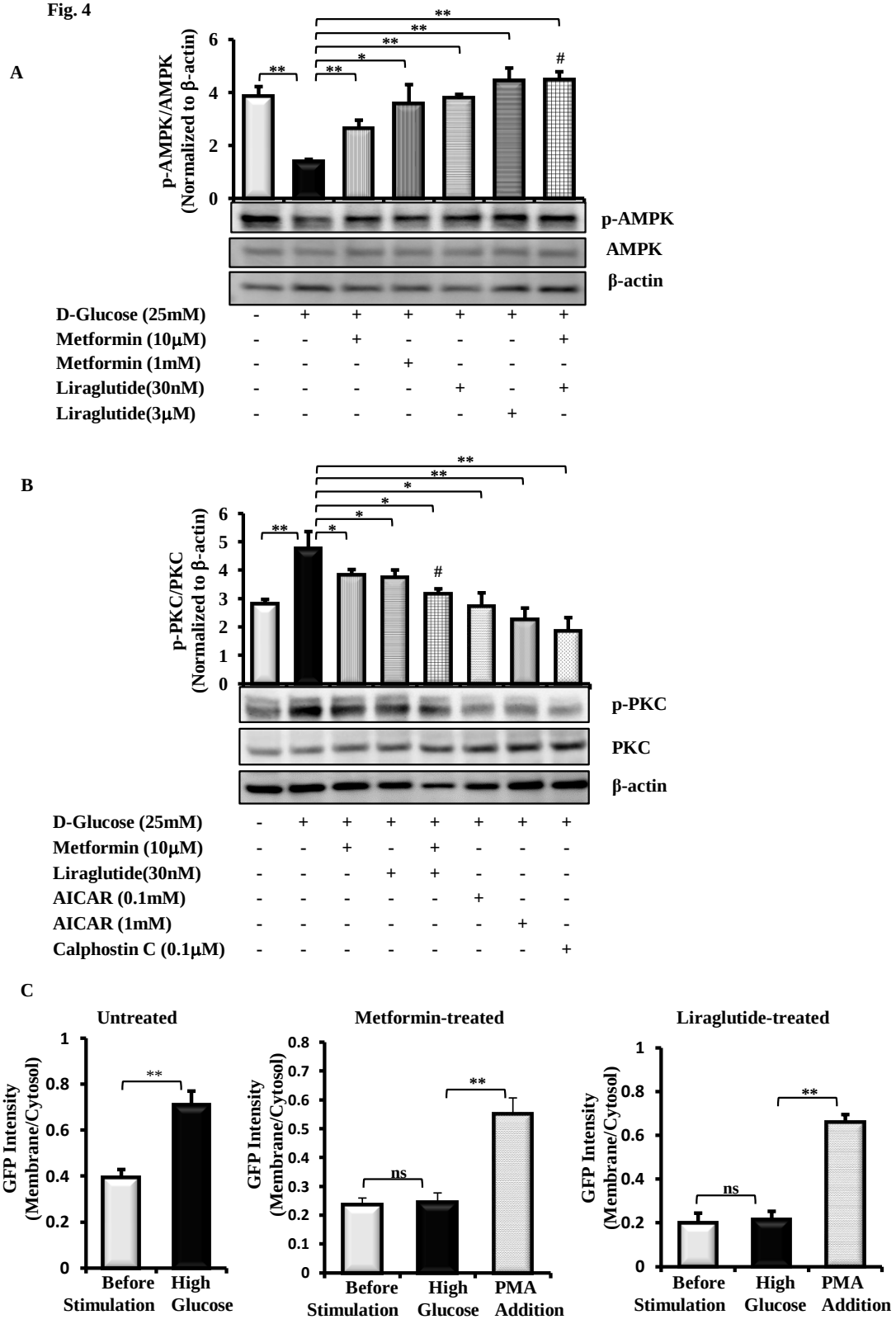
A
p-AMPK/AMPK
(Normalized to β-actin)
p-AMPK
AMPK
β-actin
D-Glucose (25mM)
Metformin (10μM)
Metformin (1mM)
Liraglutide(30nM)
Liraglutide(3μM)
B
p-PKC/PKC
(Normalized to β-actin)
p-PKC
PKC
β-actin
D-Glucose (25mM)
Metformin (10μM)
Liraglutide(30nM)
AICAR (0.1mM)
AICAR (1mM)
Calphostin C (0.1μM)
C
Untreated
Metformin-treated
Liraglutide-treated
GFP Intensity
(Membrane/Cytosol)
Before Stimulation
High Glucose
PMA Addition
ns

Fig. 5

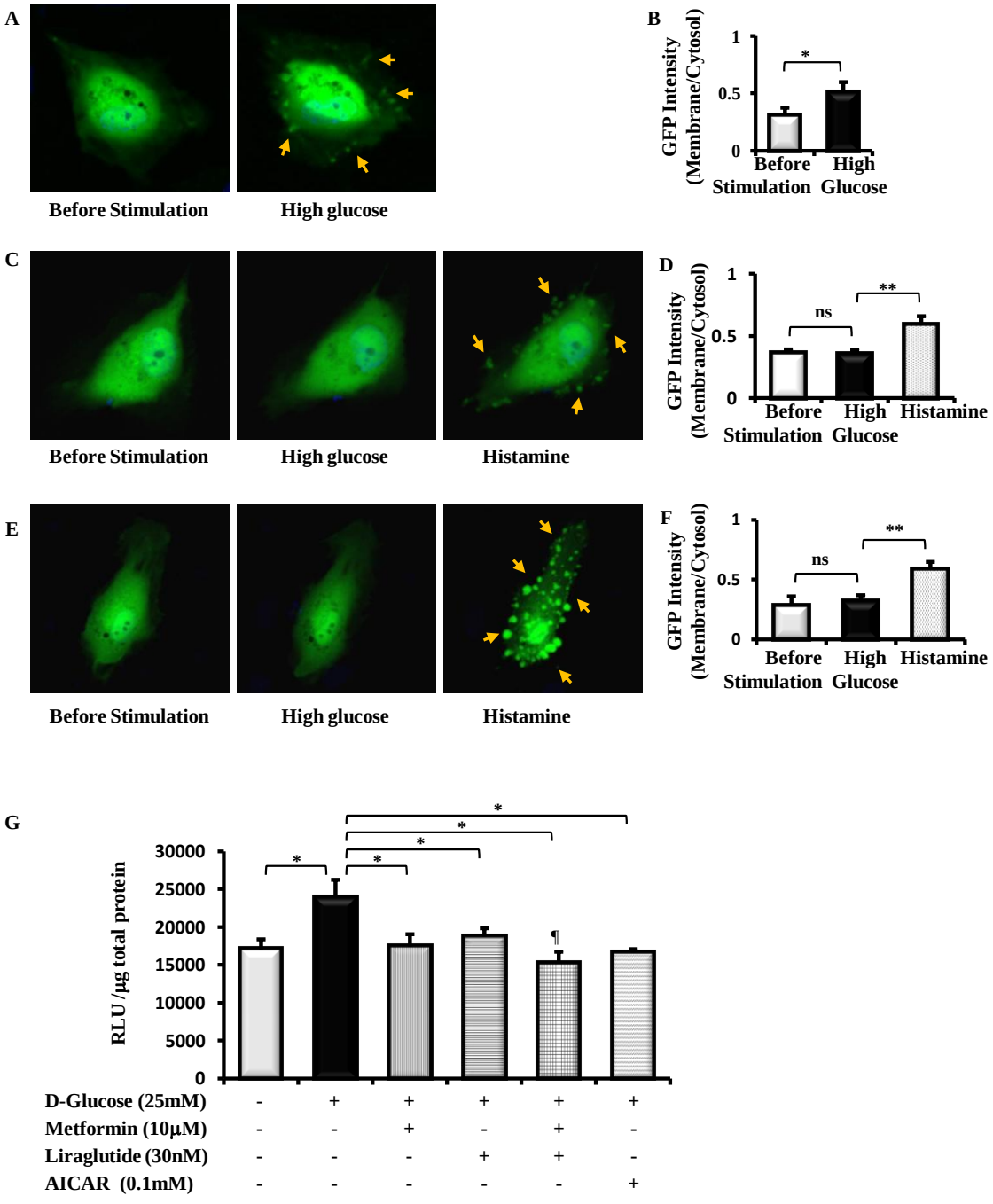
A
Before Stimulation
High glucose
B
GFP Intensity (Membrane/Cytosol)
1
0.5
0
*
Before Stimulation
High Glucose
C
Before Stimulation
High glucose
Histamine
D
GFP Intensity (Membrane/Cytosol)
1
0.5
0
ns
**
Before Stimulation
High Glucose
Histamine
E
Before Stimulation
High glucose
Histamine
F
GFP Intensity (Membrane/Cytosol)
1
0.5
0
ns
**
Before Stimulation
High Glucose
Histamine
G
RLU /μg total protein
30000
25000
20000
15000
10000
5000
0
*
¶
D-Glucose (25mM) - + + + + +
Metformin (10μM) - - + - + -
Liraglutide (30nM) - - - + + -
AICAR (0.1mM) - - - - - +